

## BEAM DYNAMICS WITH THE HAMILTON-JACOBI EQUATION\*

W. E. GABELLA

*University of Colorado, Boulder, Colorado 95064*<sup>†</sup>

R. D. RUTH, R. L. WARNOCK

*Stanford Linear Accelerator Center, Stanford University, Stanford, California 94309*

### ABSTRACT

We describe a non-perturbative method to solve the Hamilton-Jacobi equation for invariant surfaces in phase space. The problem is formulated in action-angle variables with a general nonlinear perturbation. The solution of the Hamilton-Jacobi equation is regarded as the fixed point of a map on the Fourier coefficients of the generating function. Periodicity of the generator in the independent variable is enforced with a shooting method. We present two methods for finding the fixed point and hence the invariant surface. A solution by plain iteration is economical but has a restricted domain of convergence. The Newton iteration is costly but yields solutions up to the dynamic aperture. Examples of lattices with sextupoles for chromatic correction are discussed.

### INTRODUCTION

This paper discusses a method to calculate approximate invariant surfaces (tori) for nonlinear dynamical systems. The surfaces are found from a numerical solution of the Hamilton-Jacobi equation.<sup>1-3</sup>

The theory is outlined in the next section. Several examples of solutions in two degrees of freedom are given in the following section. Finally results are summarized.

### THEORY

The Hamiltonian describing single particle motion in transverse phase space for a storage ring or synchrotron can be written in action-angle variables as,<sup>4</sup>

$$H(\Phi, \mathbf{I}, s) = \Omega(s) \cdot \mathbf{I} + V(\Phi, \mathbf{I}, s) \quad , \quad (1)$$

where  $\Omega(s) = (1/\beta_1(s), 1/\beta_2(s))$ ,  $\mathbf{I} = (I_1, I_2)$ , and  $\Phi = (\phi_1, \phi_2)$  for the two transverse dimensions. The Hamiltonian is periodic in  $s$  with periodicity  $C$ , the circumference of the ring. The perturbation considered here is due to sextupoles used for chromatic correction,

$$V(x, y, s) = \frac{S(s)}{3!} (x^3 - 3xy^2) \quad . \quad (2)$$

The perturbation is expressed in action-angle variables through the transformations

$$\begin{aligned} x &= [2I_1\beta_1(s)]^{\frac{1}{2}} \cos \phi_1 \quad , \\ p_x &= -[2I_1/\beta_1(s)]^{\frac{1}{2}} [\sin \phi_1 + \alpha_1(s) \cos \phi_1] \quad . \end{aligned} \quad (3)$$

The  $y$  and  $p_y$  have similar transformations.

To derive the Hamilton-Jacobi equation (HJE) consider a canonical transformation of the second type  $F_2$  from the old variables  $(\Phi, \mathbf{I})$  to the new variables  $(\Psi, \mathbf{J})$ :

$$F_2(\Phi, \mathbf{J}, s) = \Phi \cdot \mathbf{J} + G(\Phi, \mathbf{J}, s) \quad . \quad (4)$$

This gives the transformation equations

$$\Psi = \Phi + G_{\mathbf{J}}(\Phi, \mathbf{J}, s), \quad (5)$$

$$\mathbf{I} = \mathbf{J} + G_{\Phi}(\Phi, \mathbf{J}, s), \quad (6)$$

$$\bar{H}(\Psi, \mathbf{J}, s) = H(\Phi, \mathbf{J} + G_{\Phi}, s) + G_s. \quad (7)$$

Subscripts indicate partial differentiation. The Hamilton-Jacobi equation is just the requirement that the new Hamiltonian be independent of the new angle variables:

$$\bar{H}(\mathbf{J}, s) = \Omega \cdot (\mathbf{J} + G_{\Phi}) + G_s + V(\Phi, \mathbf{J} + G_{\Phi}, s) \quad . \quad (8)$$

Solutions to the HJE that are periodic in  $\Phi$  and  $s$  give the invariant surface  $\mathbf{I}(\Phi, s; \mathbf{J})$  according to Eq. (6). The new actions  $\mathbf{J}$  are constant.

If  $G$  is represented as a Fourier series in  $\phi_1$  and  $\phi_2$ , the HJE for the Fourier coefficients  $g_{\mathbf{m}}$  for  $\mathbf{m} = (m_1, m_2) \neq 0$  is

$$\partial_s g_{\mathbf{m}} + i\Omega \cdot \mathbf{m} g_{\mathbf{m}} + V_{\mathbf{m}}(\mathbf{J}, s; g) = 0 \quad , \quad (9)$$

where the vector of Fourier coefficients is written  $g = \{g_{\mathbf{m}}\}$  and

$$\begin{aligned} V_{\mathbf{m}}(\mathbf{J}, s; g) &= \int \frac{d^2\Phi}{(2\pi)^2} e^{-i\mathbf{m} \cdot \Phi} V(\Phi, \mathbf{J} + G_{\Phi}, s) \quad , \\ G_{\Phi}(\Phi, \mathbf{J}, s) &= \sum_{\mathbf{m} \in S} i\mathbf{m} g_{\mathbf{m}}(\mathbf{J}, s) e^{i\mathbf{m} \cdot \Phi} \quad . \end{aligned} \quad (10)$$

The set of modes used for the numerical calculation is  $S$ .

The first two terms of Eq. (9) can be consolidated by using the integrating factor  $e^{i\mathbf{m} \cdot \chi}$ , where  $\chi_i(s) = \int_0^s du/\beta_i(u)$  is the phase advance. The new vector  $h_{\mathbf{m}} = e^{i\mathbf{m} \cdot \chi(s)} g_{\mathbf{m}}$  is the solution to

$$\partial_s h_{\mathbf{m}} = -e^{i\mathbf{m} \cdot \chi(s)} V_{\mathbf{m}}(\mathbf{J}, s; g(h)) \quad . \quad (11)$$

Note that the  $h_{\mathbf{m}}$  are constant between nonlinear elements. They have a modified periodicity  $h_{\mathbf{m}}(C) = e^{2\pi i \mathbf{m} \cdot \nu} h_{\mathbf{m}}(0)$  which follows from  $g_{\mathbf{m}}(C) = g_{\mathbf{m}}(0)$ .

The numerical integration of Eq. (11) from an initial value is the map  $U$  on the initial conditions

$$h(C) - h(0) = U(h(0)) \quad . \quad (12)$$

The periodicity of the  $h(s)$  and Eq. (12) define a boundary value problem

$$\begin{aligned} h_{\mathbf{m}}(0) &= \frac{1}{e^{2\pi i \mathbf{m} \cdot \nu} - 1} U_{\mathbf{m}}(h(0)) \\ &= A_{\mathbf{m}}(h(0)) \quad . \end{aligned} \quad (13)$$

The solution to Eq. (13) is the fixed point of the map  $A(h)$  and is constructed to be the periodic solution to the original differential equation, Eq.(11). This fixed point is found by simple iteration for small betatron amplitudes and by Newton's iteration<sup>5</sup> at large amplitudes near unstable regions of phase space.

\* Work supported by the Department of Energy contracts DE-FG02-86ER40302 (Colorado) and DE-AC03-76SF00515 (SLAC).

†Current address SLAC, Stanford University, Stanford, California 94309.

TABLE I — Single Cell of the ALS									
C=16.4m, 1/12 of ring, $\nu_x=1.18973$ , $\nu_y=0.68158$									
Parameters at beginning of element									
NAME	POSITION	STRENGTH	LENGTH	TWISS PARAMETERS				PHASE	
				$\beta_{1,m}$	$\beta_{2,m}$	$\alpha_1$	$\alpha_2$	$\psi_1, \text{rads}$	$\psi_2, \text{rads}$
SD	5.775	-88.090	.20	1.472	10.696	-1.779	8.401	2.480	0.866
SF	6.875	115.615	.20	3.984	1.580	2.272	0.417	2.819	1.222
SF	9.325	115.615	.20	3.137	1.443	-1.963	-0.268	4.600	2.928
SD	10.425	-88.090	.20	2.297	7.603	2.345	-7.062	4.886	3.395

In Newton's method  $F(h) = h - A(h) = 0$  is solved by the iteration

$$0 = F_m(h^i) + \sum_n D_{mn}(h^i) \cdot (h^{i+1} - h^i)_n. \quad (14)$$

The Jacobian of the map is  $D_{mn} = \partial F_m / \partial h_n$ . Its calculation by divided differences is adequate but requires two evaluations of the map for each independent, complex Fourier amplitude. In two dimensions, the number of independent amplitudes is  $2M_1M_2 + M_1 + M_2$  if modes are chosen for  $|m_i| \leq M_i$  with  $i = 1, 2$ . At typical values of  $M_i = 16$  this gives an excessive number of modes.

However using Broyden's formula<sup>6-7</sup> to update the Jacobian, and selecting only the numerically significant modes for the mode set  $S$  reduces the computation time. Broyden's formula gives an estimate for the Jacobian  $D^{i+1}$  at the next iteration given the Jacobian  $D^i$  at  $h^i$ .

$$D^{i+1} = D^i + \frac{[F(h^{i+1}) - F(h^i) - D^i(h^{i+1} - h^i)](h^{i+1} - h^i)^T}{\|h^{i+1} - h^i\|^2}. \quad (15)$$

The resulting Newton-Broyden iteration does not converge as fast as the real Newton iteration, but it has the advantage that the next Jacobian is given after only one more evaluation of the map. Only one full divided difference calculation of the Jacobian is done at the start of the iteration.

Furthermore, using only modes that contribute significantly to the evaluation of  $G_\Phi$  reduces the number of map evaluations that must be done for the first Jacobian calculation. Modes are selected with values of  $\|mh_m\|/\|J\|$  above a cut-off. All other modes are consistently ignored.

Once the  $g_m(s_0)$  are known the invariant surface  $\mathbf{I}(\Phi, s_0; \mathbf{J})$  is given according to Eqs. (6) and (10).

### NUMERICAL RESULTS

In this section the design for a single cell of the Berkeley Advanced Light Source<sup>8</sup> (ALS) is analyzed. See Table I for parameters of the single cell design. It has been studied with the one dimensional HJE technique<sup>3</sup> but the problem is much more difficult in two dimensions because of the large number of modes.

Figure 1 is a stability diagram for the ALS cell. It gives initial positions in  $x$  and  $y$  of stable (+) and unstable (\*) trajectories. The trajectories were tracked for 5000 turns

by means of a 4th-order symplectic integration<sup>9</sup> of the equations of motion in the sextupoles. Trajectories that grew larger in amplitude than some cut-off are unstable and those that did not are stable. The points  $A$  and  $B$  correspond to the invariant surface solutions discussed below.

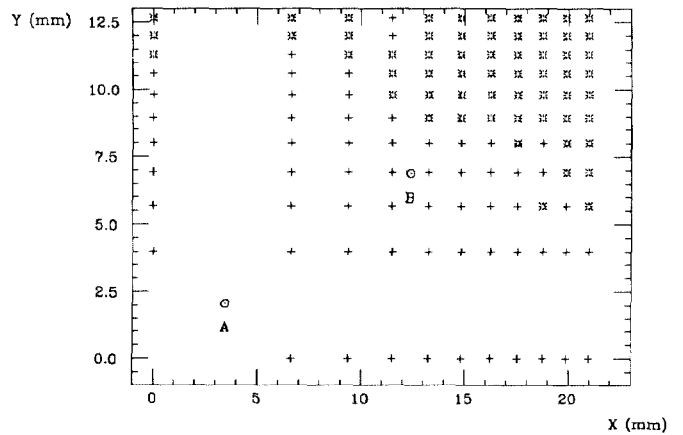


Fig. 1 Stability Diagram for single cell ALS

In case  $A$ , the invariant surface is found for the constant action  $J_1=J_2=5 \times 10^{-7}$  m. It gives initial displacements in  $(x, y)$  of 3.5mm and 2.1mm, respectively, for  $\phi_1 = \phi_2 = 0$ . A surface of section of the invariant torus, corresponding to a single value of  $s$ , is plotted<sup>10</sup> as  $I_i(\Phi, s; \mathbf{J})$  for  $i = 1, 2$ . See Figs. 2 and 3. The map is evaluated by a 4th-order Runge-Kutta algorithm using 2 steps per magnet. The mode set is selected from the set with  $|m_i| \leq 13$ , the selection criterion being  $\|mh_m\|/\|J\| \geq 10^{-6}$ . This yields 65 modes of the 364 independent modes in the truncated mode set. Convergence of the Newton-Broyden iteration is gauged with the parameter  $r_{i+1} = \|h^{i+1} - h^i\|/\|h^i\|$ , for the  $(i+1)$ -th iteration. The iteration converges quickly, by about  $6.4 \times 10^{-4}$  per iteration, to the final value of  $r_3 = 4.03 \times 10^{-12}$ . Agreement of the invariant surface with the points  $(\Phi^T, \mathbf{I}^T)$  found from the tracking code is excellent. The difference between the surface and the points was quantified as  $\delta_x = \sum_{i=1}^N |I_x^{JJ}(\Phi_i^T) - I_{xi}^T|/(NJ_x)$  and similarly for the  $y$  plot. For this case,  $\delta_x = 4.43 \times 10^{-5}$  and  $\delta_y = 4.56 \times 10^{-5}$ , with  $N = 600$ .

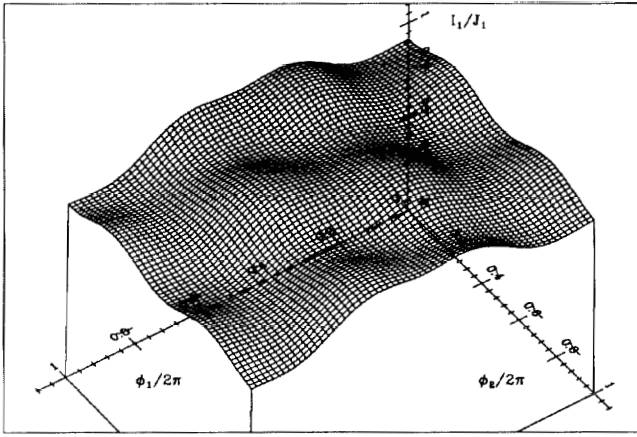


Fig. 2 Case A,  $J_1 = J_2 = 5 \times 10^{-7} \text{m}$ , X Action

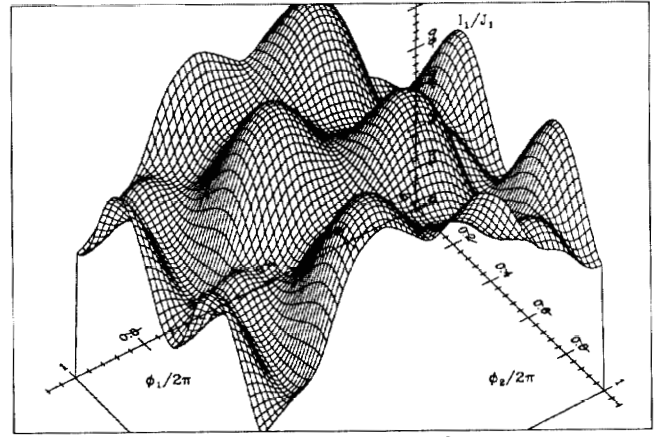


Fig. 4 Case B,  $J_1 = J_2 = 5 \times 10^{-6} \text{m}$ , X Action

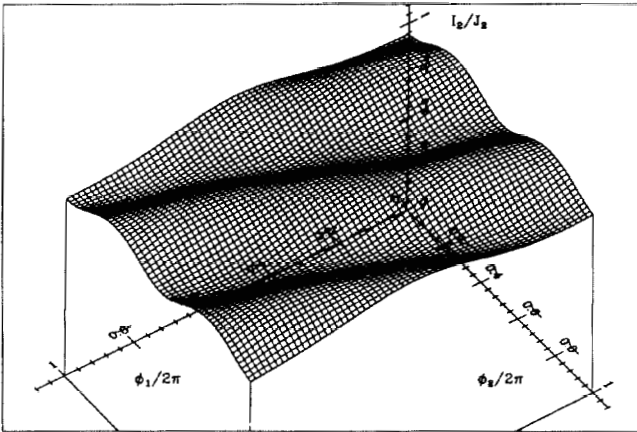


Fig. 3 Case A,  $J_1 = J_2 = 5 \times 10^{-7} \text{m}$ , Y Action

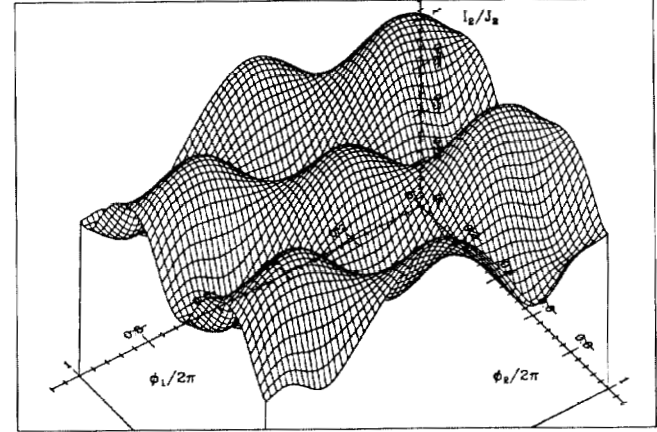


Fig. 5 Case B,  $J_1 = J_2 = 5 \times 10^{-6} \text{m}$ , Y Action

In case B, the invariant surface for  $J_1=J_2=5 \times 10^{-6} \text{m}$  gives initial displacements of 12.4mm and 6.9mm in  $(x, y)$  for  $\phi_1 = \phi_2 = 0$ . See Figs. 4 and 5 for the plots of the surface of section. This case requires more steps in the Runge-Kutta evaluation of the map and more selected modes than the previous case, as is typical of cases close to unstable regions of phase space. The evaluation of the map is performed with 6 Runge-Kutta steps per magnet. There are 127 modes selected for  $\|mh_m\|/\|J\| \geq 2 \times 10^{-5}$ . The iteration converged much more slowly than the previous case taking 14 iterations to reach  $r_{14} = 3.56 \times 10^{-13}$ , decreasing by 0.15 each iteration. Agreement with tracking is still good:  $\delta_x = 1.83 \times 10^{-3}$  and  $\delta_y = 1.66 \times 10^{-3}$ .

At small amplitudes simple iteration converges and requires much less computation time. For the above cell convergence occurs around  $J_1=J_2=5 \times 10^{-8} \text{m}$  or  $x=1 \text{mm}$ ,  $y=0.6 \text{mm}$ .

#### SUMMARY

The Hamilton-Jacobi equation was solved numerically for the invariant surface in two degrees of freedom. Several examples were given and a convenient way to plot the results was shown. For solutions at large amplitude, mode selection and Broyden updating of the Jacobian were employed to save considerable computing time.

#### ACKNOWLEDGEMENTS

One of the authors (W. E. G.) would like to thank the SLAC Accelerator Theory and Special Projects group for their kindness and hospitality.

#### REFERENCES

1. R. L. Warnock and R. D. Ruth, *Proceedings of the 1987 IEEE Particle Accelerator Conference*, Washington, D. C., March 16-19, 1987, p. 1263.
2. R. L. Warnock and R. D. Ruth, *Physica D*, **26**, 1987, pp. 1-36.
3. W. E. Gabella, R. D. Ruth, R. L. Warnock, *Proceedings of the Second ICFA Advanced Beam Dynamics Workshop*, J. Hagel and E. Keil, eds., Lugano, Switzerland, April 11-16, 1988, CERN 88-04.
4. R. D. Ruth, *Nonlinear Dynamics Aspects of Particle Accelerators*, **247**, Springer-Verlag, Berlin, 1986.
5. M. A. Krasnosel'skii et al., *Approximate Solutions of Operator Equations*, transl. by D. Louvish, Wolters-Noordhoff Publishing, Groningen, 1972, ch. 1 and ch. 3, p. 138.
6. C. G. Broyden, *Math. Comp.*, **19**, 1965, pp. 577-593.
7. M. J. D. Powell, *Proceedings of the First International Conference on Industrial and Applied Mathematics*, J. McKenna and R. Terman, eds., SIAM, Philadelphia, 1988.
8. "1-2 GeV Synchrotron Radiation Source, Conceptual Design Report - July 1986," PUB-5172 Rev., Lawrence Berkeley Laboratory, Berkeley, California.
9. R. D. Ruth, unpublished. The 3rd-order algorithm was given in R. D. Ruth, *IEEE Trans. Nucl. Sci.*, NS-30, 1983, p. 2669.
10. R. D. Ruth, T. Raubenheimer, and R. L. Warnock, *IEEE Trans. Nucl. Sci.*, NS-32, 1985, p. 2206.